



|                               |   |
|-------------------------------|---|
| <b>Publication Year</b>       | 2020  |
| <b>Acceptance in OA @INAF</b> | 2021-12-10T15:14:31Z  |
| <b>Title</b>                  | A heatwave of accretion energy traced by masers in the G358-MM1 high-mass protostar             |
| <b>Authors</b>                | Burns, R. A.; Sugiyama, K.; Hirota, T.; Kim, Kee-Tae; Sobolev, A. M.; et al.                    |
| <b>DOI</b>                    | 10.1038/s41550-019-0989-3   |
| <b>Handle</b>                 | <a href="http://hdl.handle.net/20.500.12386/31229">http://hdl.handle.net/20.500.12386/31229</a> |
| <b>Journal</b>                | NATURE ASTRONOMY  |
| <b>Number</b>                 | 4   |

# Riding the heatwave: account of the G358.93-0.03 maser flare.

R. A. Burns,<sup>1,2\*</sup> K. Sugiyama,<sup>1,3</sup> T. Hirota,<sup>1</sup> K. Kim,<sup>2</sup> A. M. Sobolev,<sup>4</sup> B. Stecklum,<sup>5</sup>  
G. C. MacLeod,<sup>6,7</sup> G. Orosz,<sup>8,9</sup> S. P. Ellingsen,<sup>8</sup> L. Hyland,<sup>8</sup> Y. Yonekura,<sup>3</sup>  
A. Caratti o Garatti,<sup>11</sup> C. Brogan,<sup>12</sup> T. Hunter,<sup>12</sup> C. Philips<sup>13</sup> J. O. Chibueze,<sup>14,15</sup> W. Baan,<sup>16</sup>  
H. Linz,<sup>17</sup> S. P. van den Heever<sup>6</sup> J. Eislöeffel,<sup>4</sup> G. Surcis,<sup>18</sup> M. Olech,<sup>19</sup> B. Kramer<sup>10,20</sup>

<sup>1</sup>Mizusawa VLBI Observatory, National Astronomical Observatory of Japan, 2-21-1 Osawa, Mitaka, Tokyo 181-8588, Japan

<sup>2</sup>Korea Astronomy and Space Science Institute, 776 Daedeokdae-ro, Yuseong-gu, Daejeon 34055, Republic of Korea

<sup>3</sup>NARIT, 260 M.4, T. Donkaew, Amphur Maerim, Chiang Mai, 50180, Thailand

<sup>4</sup>Ural Federal University, 19 Mira St. 620002, Ekaterinburg, Russia

<sup>5</sup>Thüringer Landessternwarte, Sternwarte 5, 07778 Tautenburg, Germany

<sup>6</sup>The University of Western Ontario, 1151 Richmond Street. London, ON N6A 3K7, Canada

<sup>7</sup>Hartebeesthoek Radio Astronomy Observatory, PO Box 443, Krugersdorp, 1741, South Africa

<sup>8</sup>School of Natural Sciences, University of Tasmania, Private Bag 37, Hobart, Tasmania 7001, Australia

<sup>9</sup>Xinjiang Astronomical Observatory, Chinese Academy of Sciences, 150 Science 1-Street, Urumqi, Xinjiang 830011, China

<sup>10</sup>Center for Astronomy, Ibaraki University, 2-1-1 Bunkyo, Mito, Ibaraki 310-8512, Japan

<sup>11</sup>Dublin Institute for Advanced Studies, Astronomy & Astrophysics Section, 31 Fitzwilliam Place, Dublin 2, Ireland

<sup>12</sup>NRAO, 520 Edgemont Rd, Charlottesville, VA, 22903, USA

<sup>13</sup>Australia Telescope National Facility, CSIRO, PO Box 76, Epping NSW 1710, Australia

<sup>14</sup>Space Research Unit, Physics Department, North West University, Potchefstroom 2520, South Africa

<sup>15</sup>Department of Physics and Astronomy, Faculty of Physical Sciences, University of Nigeria, Carver Building,

1 University Road, Nsukka, Nigeria

<sup>16</sup>Netherlands Institute for Radio Astronomy, Dwingeloo, The Netherlands

<sup>17</sup>Max Planck Institute for Astronomy, Königstuhl 17, 69117 Heidelberg, Germany

<sup>18</sup>INAF Osservatorio Astronomico di Cagliari, Via della Scienza 5, 09047 Selargius, Italy

<sup>19</sup>Centre for Astronomy, Faculty of Physics, Astronomy and Informatics, Nicolaus Copernicus University, Grudziadzka 5,

87-100 Torun, Poland

<sup>20</sup>Max-Planck-Institut für Radioastronomie, Auf dem Hügel 69, 53121 Bonn, Germany

High-mass stars are thought to accumulate much of their mass via short, infrequent bursts of disk-aided accretion [1; 2]. Such accretion events are rare and difficult to observe directly but are known to drive enhanced maser emission [3; 4]. In this Letter we report high-resolution, multi-epoch methanol maser observations toward G358.93-0.03 which reveal a new phenomenon; the sub-luminal propagation of a thermal radiation "heat-wave" emanating from an accreting high-mass proto-star. The extreme transformation of the maser emission implies a sudden intensification of thermal infrared radiation from within the inner (40 mas, 270 au) region. Subsequently, methanol masers trace the radial passage of thermal radiation through the environment at 4-8% the speed of light. Such a high translocation rate contrasts with the  $\leq 10 \text{ km s}^{-1}$  physical gas motions typically observed with VLBI arrays. This scenario can readily be attributed to an accretion event in the high-mass proto-star G358.93-0.03-MM1. While being the third case in its class, G358.93-0.03-MM1 exhibits unique attributes hinting at a possible 'zoo' of accretion burst types. These results promote the advantages of maser observations in understanding high-mass star formation, both through single-dish maser monitoring campaigns and via their international cooperation as VLBI arrays.

(end of introductory paragraph: 190 words)

48 Masers provide a novel approach to investigating accretion bursts [3; 4]. **The  $5_1 \rightarrow 6_0 A^+$**   
 49 **methanol transition at 6.7 GHz being of particular suitability as it arises in the**  
 50 **presence of far-infrared radiation from warm ( $>100$  K) dust and high gas densities**  
 51 **( $10^{5-8} \text{ cm}^{-3}$ ) [5], making it a sign-post of high-mass star formation [6]. It has been**  
 52 **seen to trace rotating disks and tori [7; 8; 9], and actively responds to changes in**  
 53 **its local environment [10].**

54 G358.93-0.03 was discovered by its 6.7 GHz methanol maser in the Methanol Multibeam  
 55 survey [11], conducted in 2006. The early 6.7 GHz spectrum showed several  $< 10$  Jy peaks in  
 56 the velocity range of  $-22.0$  to  $-14.5 \text{ km s}^{-1}$ . In January 2019 a flare of the 6.7 GHz methanol maser  
 57 at  $-15.9 \text{ km s}^{-1}$  was identified [12] using the Hitachi 32m telescope [13], prompting intensive  
 58 monitoring and follow-up observations across a wide range of facilities. These observations,  
 59 coordinated by the Maser Monitoring Organisation (M2O<sup>1</sup>) constitute the first observational  
 60 campaign conducted *during* an accretion burst in a high-mass star.

61 Early results from target of opportunity observations with the SMA, ALMA [14] the ATCA  
 62 [15], the VLA [16; 17] **and SOFIA [18]** have already been established. These contemporary  
 63 works have revealed striking temporal behavior [19; 14], rich and dynamic hot core chemistry  
 64 [15; 14], complex maser emission [14; 17; 16] **and a kinematic signature indicating possible**  
 65 **expansion [14].** The (sub)mm dust continuum uncovered a cluster environment, with the  
 66 most luminous source ( $L_{\text{bol}} = 5700 - 22000 L_{\odot}$ ), G358.93-0.03-MM1 (hereafter "G358-MM1"),  
 67 being the counterpart to the aforementioned flare activity [14]. **An enhancement in the far**  
 68 **infrared continuum of this source confirms that an accretion burst has occurred**  
 69 **[18].**

70 Using hot core thermal tracers [14] adopt a line of sight velocity in the Local Standard of Rest  
 71 of  $v_{\text{LSR}} = -16.5 \pm 0.3 \text{ km s}^{-1}$ , and estimate a kinematic distance of  $D = 6.75^{+0.37}_{-0.68}$  kpc using a  
 72 Bayesian statistics Galactic distance estimation tool [20]. Gaia parallaxes of visible stars within  
 73 a 0.25 arcminute field around G358 had distance estimates within 5 kpc [21]. Assuming that  
 74 such stars are foreground to the G358 high-mass star forming region imposes a lower distance  
 75 limit which is consistent with the kinematic distance.

76 **As part of the M2O-lead campaign we initiated VLBI (very long baseline inter-**  
 77 **ferometry) observations to contribute the highest angular resolution view of masers**  
 78 **during the G358-MM1 maser flare. Two VLBI observations of the 6.7 GHz methanol**  
 79 **maser were conducted with the Australian long baseline array (LBA) shortly fol-**  
 80 **lowing the discovery of the maser burst (see Methods). Spectral profiles delineating**  
 81 **both auto- and cross-correlations for each epoch are presented in Figure 1, in which**  
 82 **emission is appears in the velocity range of  $-14.3$  to  $-20.5 \text{ km s}^{-1}$ ; centered near the**  
 83 **source systemic velocity [14].**

84 Auto-correlation spectra are sensitive to all emission within the arcminute scale  
 85 primary beams of the VLBI array elements. Contrarily, cross-correlation spectra  
 86 are exclusively sensitive to compact gas, on scales similar to the VLBI array synthe-  
 87 sised beam (a few milliarcseconds). The similarity of the auto- and cross-correlation  
 88 spectral profiles implies a common origin and similar spatio-kinematics of the maser  
 89 gas at both extended and compact scales. Comparison of the auto-correlation and  
 90 cross-correlation flux densities indicate that at least 90% of the maser emission in  
 91 G358-MM1 originates from gas at angular scales larger than the synthesised beam  
 92 of the LBA (see Table 1). Generally, maser emission in G358-MM1 rapidly evolves toward  
 93 a more complex spectral profile with most features increasing in flux density by several times  
 94 their initial values.

95 Phase referenced, astrometric positions of the masers around G358-MM1 are shown in Fig-  
 96 ure 2, in which the white cross indicates the peak of the millimeter core detected by ALMA at  
 97 (RA, DEC) = (17:43:10.1014, -29:51:45.693; [14]). Despite significant changes across the two

<sup>1</sup>The M2O is a global co-operative of maser monitoring programs. <https://MaserMonitoring.org>

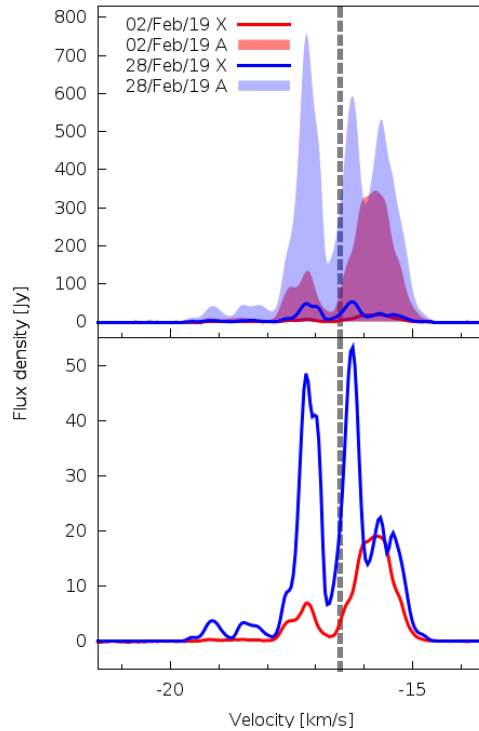


Figure 1: Spectral profiles of the 6.7 GHz methanol maser emission in G358-MM1. *Above* depicts a comparison of the auto- and cross-correlation profiles with the cross-correlation data shown *below*. The dashed line indicates the source systemic velocity.

98 epochs, the 6.7 GHz methanol maser emission in G358-MM1 is generally arranged in a ring-like  
 99 structure roughly centered on the position of the millimeter core. By the very nature of maser  
 100 emission detections are biased toward regions of longest velocity-coherent path length along  
 101 the line of sight. As such, the ring-like structures likely represent 2D projections of a 3D shell  
 102 centered on G358-MM1.

103 The most striking aspect of the VLBI data is the rapid transformation of the methanol maser  
 104 distribution. Circles fit to the spot maps (Figure 3 *right*) delineate radii of 40 mas and 77 mas  
 105 (260 and 520 au) in the first and second epochs respectively, corresponding to a translocation of  
 106 1 mas/day in the NW direction, 2 mas/day in the SE direction and an average radial expansion  
 107 of 1.5 mas/day generally progressing outward from a position near the MM1 continuum peak  
 108 [14].

109 Considering the short period between observations (26 days), spatial evolution of the maser  
 110 emission must be dominated by local phenomena ( $\sim$  mas/day) with no significant contribution  
 111 expected from Galactic systemic apparent proper motions ( $\sim$  mas/yr).

112 **Translocation rates of 1-2 mas/day, correspond** to 11,700 to 23,400 km s<sup>-1</sup> at the  
 113 source's kinematic distance of 6.75 kpc, equivalent to 0.04 to 0.08c. Methanol does not achieve  
 114 high gas phase abundance in the presence of shocks faster than 10 km s<sup>-1</sup> [22], therefore such  
 115 a fast morphological transformation can not be attributed to physical motions of methanol gas  
 116 clouds. Instead, it is suitably explained by the sequential creation and quenching of maser  
 117 emitting regions at ever increasing radii, as the conditions favorable to maser production [5]  
 118 propagate outward from an origin at G358-MM1.

119 A sudden production and subsequent propagation of thermal heating, **emanating from** the  
 120 inner 270 au region in G358-MM1, can readily be explained under the hypothesis of an accretion  
 121 event **in which enhanced far infrared radiation drives the production of  $5_1 \rightarrow 6_0 A^+$**   
 122 **methanol masers..** The propagation progresses as a random-walk of the energy transfer by  
 123 dust absorption and re-emission. The mean free path of photons becomes small at high optical  
 124 depths, and energy absorption in the melting of ice mantles can further slow radiative transfer,  
 125 leading to subluminal propagation (see [23]).

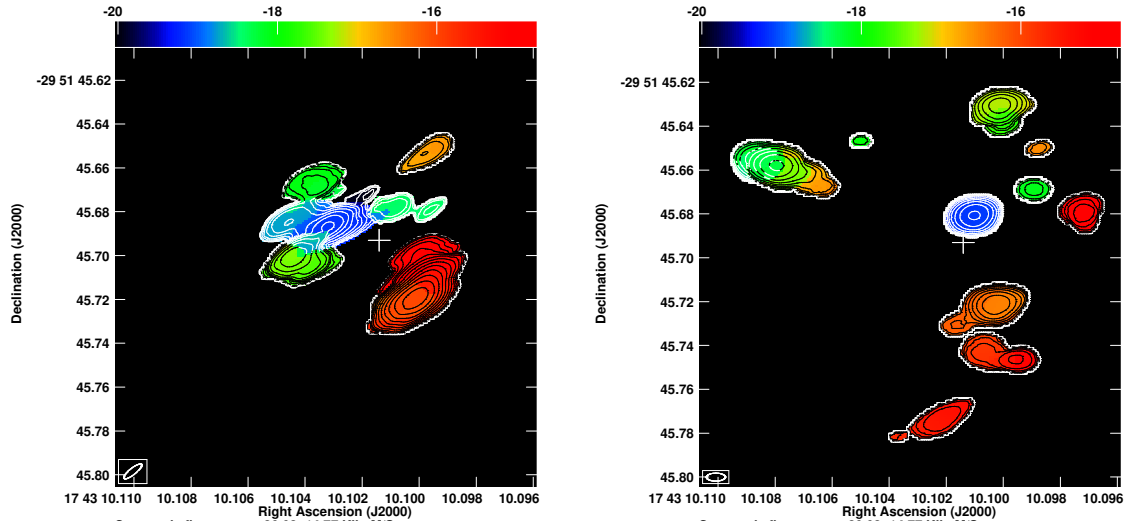


Figure 2: Zero'th (contours) and first (colours) moment maps of the 6.7 GHz methanol maser emission in G358-MM1. *Left* shows the distribution of emission during the VX026A epoch while *right* shows that of VX026C, taken 26 days later. Contours increase by factors of 2 multiples of the first contour at  $2 \text{ Jy beam}^{-1} \text{ km s}^{-1}$ . The white cross indicates the position of the brightest millimeter continuum peak of the G358-MM1 region from [14].

126 **Alternative explanations for the phenomena seen in G358-MM1, including super-**  
 127 **/nova and changes in the geometry and/or radiation of a high-mass protostellar**  
 128 **system, fail to explain the global flux increase in all velocity components of the**  
 129 **maser emission, its temporal behavior and rapid morphological changes, and the**  
 130 **accompanying FIR enhancement. All of which are consistent with the accretion**  
 131 **burst hypothesis.**

132 High-mass protostars may be facilitated in achieving their necessarily high accretion rates  
 133 by disk-aided inward transport of material and a reduction of the stellar UV radiation. The  
 134 latter may be induced via non-continuous accretion mechanisms [24] which cause a bloating of  
 135 the stellar radius and a subsequent reduction in its effective temperature [25]. Such ‘episodic  
 136 accretion’ is exemplified by the FUori and EXori class of low-mass protostars (reviewed in  
 137 [24]) and, **despite differences in the initial conditions, timescales, environments and**  
 138 **protostellar radiation fields present in low- and high-mass protostars [26], episodic**  
 139 **accretion** is quickly becoming considered a necessary component of high-mass star formation  
 140 [1; 2]. Accretion bursts were identified retrospectively in high-mass protostars S255NIRS3 [27]  
 141 and NGC6334I-MM1 [28] and the behavior has been inferred indirectly via outflow ejection  
 142 histories[29].

143 **The G358-MM1 accretion burst contrasts to the those of S255NIRS3 [27] and**  
 144 **NGC6334I-MM1 [28] in that no clear enhancements in the near- and mid-infrared,**  
 145 **were confirmed [14; 18]. The former can be explained by a high opacity in the**  
 146 **immediate surroundings of the high-mass protostar, and the latter implying a sub-**  
 147 **sequent failure to sufficiently heat the dust in the disk mid-plane. This may be**  
 148 **due to a less substantial mass transfer, leading to less intense accretion luminosity.**  
 149 **Indeed, S255NIRS3 exhibited a bolometric luminosity increase of a factor of 4 while**  
 150 **that of NGC6334I increased by a of 10, despite a common underlying mechanism.**  
 151 **The G358-MM1 event may therefore represent a new discovery amongst a ‘zoo’ of**  
 152 **high-mass protostar accretion burst varieties. It is likely that this class of events**  
 153 **will diversify as more follow-up investigations of accretion bursts are reported.**

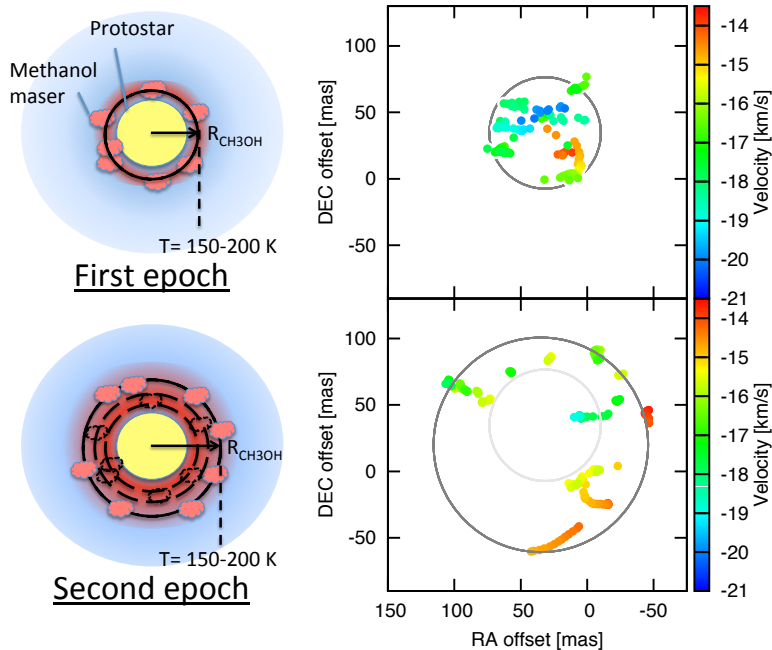


Figure 3: (Left) A schematic model of the maser distribution and evolution in an accreting star-disk system. Right Spot maps detailing the evolution of methanol maser emission in G358-MM1 where the upper and lower panels illustrate the data of VX026A (2nd Feb 2019) and VX026C (28th Feb 2019), respectively. Directional offsets are stated with respect to the coordinate (RA, DEC) = (17:43:10.1014, -29:51:45.693). The dark rings delineate the fits to each epoch, while the grey ring indicates the extent of the VX026A masers at the epoch of VX026C.

## 155 Methods

156 Target of opportunity observations were requested to the Australian long baseline array (LBA)<sup>2</sup>  
 157 on January the 28th 2019 in response to reports from the M2O of the 6.7 GHz burst event [12].  
 158 Two VLBI epochs were granted. The array parameters for which are described in Table 1

159 Observations consisted of phase reference cycles between G358-MM1 and two phase reference  
 160 sources, J1744-3116 and J1743-3058, interchangeably, with a 4.5 min cycle time. Each hour,  
 161 scans were made of bright calibration sources 3C273, PKS B1934-638, NRAO530, which were  
 162 also used to phase-up the ATCA. Two 16 MHz channels of dual circular polarisation data were  
 163 recorded with 2 bit, Nyquist sampling, corresponding to a data rate of 128 Mbps. Data were  
 164 correlated with a 2 second accumulation period at the Pawsey correlator center using DiFX  
 165 [30]. Two passes were performed, one comprising the full bandwidth correlated at 32 spectral  
 166 points per channel, and one single ‘zoom band’ of 4 MHz, centered on the maser peak, with  
 167 4096 spectral points corresponding to frequency and velocity spacings of 0.977 kHz, and 0.045  
 168  $\text{km s}^{-1}$ . Full Stokes correlation products were computed.

169 Data were calibrated using the AIPS software package<sup>3</sup>. Individual station gains were cali-  
 170 brated by scaling the auto-correlation spectrum of the maser to match contemporaneous moni-  
 171 toring data provided by the M2O. Absolute flux density calibration is considered accurate to  
 172 20%. Bandpass subtracted auto- and cross-correlated spectra for both epochs are shown in  
 173 Figure 1.

174 Delay calibration was performed using 3C273, PKS B1934-638 and NRAO530 and solutions  
 175 applied to all sources. Phase calibration was established using the maser data and refined by self  
 176 calibration to remove the effects of source structure. The solutions were then applied to J1744-  
 177 3116 and J1743-3058, thereby establishing the coordinates of the maser source with respect

<sup>2</sup>The Long Baseline Array is part of the Australia Telescope National Facility which is funded by the Australian Government for operation as a National Facility managed by CSIRO.

<sup>3</sup>Astronomical Image Processing System, <http://www.aips.nrao.edu/index.shtml>

178 to the International Celestial Reference Frame to within  $\pm 3$  milli-arcseconds (mas). During  
 179 imaging the data were weighted to produce a comparable synthesised beam shape across the  
 180 two epochs. Zero'th and first moment maps (Figure 2) were produced for both epochs in which  
 181 a channel dependent noise cutoff was applied to remove any side-lobe emission. Finally, two  
 182 dimensional Gaussian functions were fit to each maser emitting region to produce the spot maps  
 183 shown in Figure 3.

Table 1: Summary of the observations

| Obs. code | Obs. date   | Duration [hrs] | Stations   | Synth. beam [mas]   |
|-----------|-------------|----------------|--|---------------------|
| VX026A    | 2 Feb 2019  | 11             | ATCA, Ceduna, Hartebeesthoek<br>Hobart, Mopra, Warkworth | $10.17 \times 2.96$ |
| VX026C    | 28 Feb 2019 | 13             | ATCA, Ceduna, Parkes<br>Hobart, Mopra, Warkworth         | $8.56 \times 3.64$  |

## 184 Acknowledgements

185 RB acknowledges support through the EACOA Fellowship from the East Asian Core Observa-  
 186 tories Association.

187 This work was supported by JSPS KAKENHI Grant Number JP19K03921. TH is financially  
 188 supported by the MEXT/JSPS KAKENHI Grant Numbers 16K05293 and 17K05398.

189 SPE, GO and LH acknowledge the support of ARC Discovery Project (project number  
 190 DP180101061).

191 This work was supported by resources provided by the Pawsey Supercomputing Centre with  
 192 funding from the Australian Government and the Government of Western Australia.

## 193 References

- 194 [1] D. Stamatellos, A. P. Whitworth and D. A. Hubber, *The Importance of Episodic Accretion for*  
 195 *Low-mass Star Formation*, *ApJ* **730** (2011) 32 [1103.1378].
- 196 [2] D. M.-A. Meyer, E. I. Vorobyov, R. Kuiper and W. Kley, *On the existence of accretion-driven*  
 197 *bursts in massive star formation*, *MNRAS* **464** (2017) L90 [1609.03402].
- 198 [3] T. R. Hunter, C. L. Brogan, G. C. MacLeod, C. J. Cyganowski, J. O. Chibueze, R. Friesen et al.,  
 199 *The Extraordinary Outburst in the Massive Protostellar System NGC 6334I-MM1: Emergence of*  
 200 *Strong 6.7 GHz Methanol Masers*, *ApJ* **854** (2018) 170 [1801.02141].
- 201 [4] G. C. MacLeod, D. P. Smits, S. Goedhart, T. R. Hunter, C. L. Brogan, J. O. Chibueze et al., *A*  
 202 *masing event in NGC 6334I: contemporaneous flaring of hydroxyl, methanol, and water masers*,  
 203 *MNRAS* **478** (2018) 1077 [1804.05308].
- 204 [5] D. M. Cragg, A. M. Sobolev and P. D. Godfrey, *Models of class II methanol masers based on*  
 205 *improved molecular data*, *MNRAS* **360** (2005) 533 [astro-ph/0504194].
- 206 [6] S. L. Breen, S. P. Ellingsen, J. L. Caswell and B. E. Lewis, *1.2-GHz methanol masers towards*  
 207 *1.2-mm dust clumps: quantifying high-mass star formation evolutionary schemes*, *MNRAS* **401**  
 208 (2010) 2219 [0910.1223].
- 209 [7] A. Bartkiewicz, M. Szymczak, H. J. van Langevelde, A. M. S. Richards and Y. M. Pihlström, *The*  
 210 *diversity of methanol maser morphologies from VLBI observations*, *A&A* **502** (2009) 155  
 211 [0905.3469].
- 212 [8] A. Bartkiewicz, M. Szymczak and H. J. van Langevelde, *European VLBI Network imaging of 6.7*  
 213 *GHz methanol masers*, *A&A* **587** (2016) A104 [1601.03197].
- 214 [9] S. P. Ellingsen, *Methanol Masers: Reliable Tracers of the Early Stages of High-Mass Star*  
 215 *Formation*, *ApJ* **638** (2006) 241 [astro-ph/0510218].
- 216 [10] K. Fujisawa, N. Aoki, Y. Nagadomi, S. Kimura, T. Shimomura, G. Takase et al., *Observations of*  
 217 *the bursting activity of the 6.7 GHz methanol maser in G33.641-0.228*, *PASJ* **66** (2014) 109  
 218 [1408.3695].
- 219 [11] J. L. Caswell, G. A. Fuller, J. A. Green, A. Avison, S. L. Breen, K. J. Brooks et al., *The 6-GHz*  
 220 *methanol multibeam maser catalogue - I. Galactic Centre region, longitudes 345 to 6*, *MNRAS* **404**  
 221 (2010) 1029 [1002.2475].

- 222 [12] K. Sugiyama, Y. Saito, Y. Yonekura and M. Momose, *Bursting activity of the 6.668-GHz CH<sub>3</sub>OH*  
223 *maser detected in G 358.93-00.03 using the Hitachi 32-m*, *ATEL* **12446** (2019) .
- 224 [13] Y. Yonekura, Y. Saito, K. Sugiyama, K. L. Soon, M. Momose, M. Yokosawa et al., *The Hitachi*  
225 *and Takahagi 32 m radio telescopes: Upgrade of the antennas from satellite communication to*  
226 *radio astronomy*, *PASJ* **68** (2016) 74.
- 227 [14] C. L. Brogan, T. R. Hunter, A. P. M. Towner, B. A. McGuire, G. C. MacLeod, M. A. Gurwell  
228 et al., *Sub-arcsecond (Sub)millimeter Imaging of the Massive Protocluster G358.93-0.03:*  
229 *Discovery of 14 New Methanol Maser Lines Associated with a Hot Core*, *ApJL* **881** (2019) L39  
230 [1907.02470].
- 231 [15] S. L. Breen, A. M. Sobolev, J. F. Kaczmarek, S. P. Ellingsen, T. P. McCarthy and M. A.  
232 Voronkov, *Discovery of Six New Class II Methanol Maser Transitions, Including the Unambiguous*  
233 *Detection of Three Torsionally Excited Lines toward G 358.9310.030*, *ApJ* **876** (2019) L25  
234 [1904.06853].
- 235 [16] X. Chen et al., *Submitted to, Nature Astronomy* (2019) .
- 236 [17] O. Bayandina et al., *in prep.*, , (2019) .
- 237 [18] B. Stecklum et al., *in prep.*, , (2019) .
- 238 [19] G. C. MacLeod et al., *Submitted to, MNRAS* (2019) .
- 239 [20] M. J. Reid, T. M. Dame, K. M. Menten and A. Brunthaler, *A Parallax-based Distance Estimator*  
240 *for Spiral Arm Sources*, *ApJ* **823** (2016) 77 [1604.02433].
- 241 [21] C. A. L. Bailer-Jones, J. Rybizki, M. Fouesneau, G. Mantelet and R. Andrae, *Estimating Distance*  
242 *from Parallaxes. IV. Distances to 1.33 Billion Stars in Gaia Data Release 2*, *AJ* **156** (2018) 58  
243 [1804.10121].
- 244 [22] G. Garay, D. Mardones, L. F. Rodríguez, P. Caselli and T. L. Bourke, *Methanol and Silicon*  
245 *Monoxide Observations toward Bipolar Outflows Associated with Class 0 Objects*, *ApJ* **567** (2002)  
246 980.
- 247 [23] B. Stecklum, A. Caratti o Garatti, K. Hodapp, H. Linz, L. Moscadelli and A. Sanna, *Infrared*  
248 *variability, maser activity, and accretion of massive young stellar objects*, in *Astrophysical Masers:*  
249 *Unlocking the Mysteries of the Universe* (A. Tarchi, M. J. Reid and P. Castangia, eds.), vol. 336 of  
250 *IAU Symposium*, pp. 37–40, Aug., 2018, 1711.01489, DOI.
- 251 [24] M. Audard, P. Ábrahám, M. M. Dunham, J. D. Green, N. Grosso, K. Hamaguchi et al., *Episodic*  
252 *Accretion in Young Stars, Protostars and Planets VI* (2014) 387 [1401.3368].
- 253 [25] T. Hosokawa, H. W. Yorke and K. Omukai, *Evolution of Massive Protostars Via Disk Accretion*,  
254 *ApJ* **721** (2010) 478 [1005.2827].
- 255 [26] J. C. Tan, *Comparison of Low-Mass and High-Mass Star Formation*, in *From Interstellar Clouds*  
256 *to Star-Forming Galaxies: Universal Processes?* (P. Jablonka, P. André and F. van der Tak, eds.),  
257 vol. 315 of *IAU Symposium*, pp. 154–162, Jan, 2016, 1510.08021, DOI.
- 258 [27] A. Caratti o Garatti, B. Stecklum, R. Garcia Lopez, J. Eislöffel, T. P. Ray, A. Sanna et al.,  
259 *Disk-mediated accretion burst in a high-mass young stellar object*, *Nature Physics* **13** (2017) 276  
260 [1704.02628].
- 261 [28] T. R. Hunter, C. L. Brogan, G. MacLeod, C. J. Cyganowski, C. J. Chandler, J. O. Chibueze et al.,  
262 *An Extraordinary Outburst in the Massive Protostellar System NGC6334I-MM1: Quadrupling of*  
263 *the Millimeter Continuum*, *ApJL* **837** (2017) L29 [1701.08637].
- 264 [29] R. A. Burns, T. Handa, T. Nagayama, K. Sunada and T. Omodaka, *H<sub>2</sub>O masers in a jet-driven*  
265 *bow shock: episodic ejection from a massive young stellar object*, *MNRAS* **460** (2016) 283.
- 266 [30] A. T. Deller, S. J. Tingay, M. Bailes and C. West, *DiFX: A Software Correlator for Very Long*  
267 *Baseline Interferometry Using Multiprocessor Computing Environments*, *PASP* **119** (2007) 318  
268 [astro-ph/0702141].